IEEE Access
Multidisciplinary ⋮ Rapid Review ⋮ Open Access Journal

Received September 19, 2019, accepted October 1, 2019, date of publication October 3, 2019, date of current version October 18, 2019.

Digital Object Identifier 10.1109/ACCESS.2019.2945475

Optimal Placement of Inertia and Primary Control: A Matrix Perturbation Theory Approach

LAURENT PAGNIER[1,2], (Member, IEEE), AND PHILIPPE JACQUOD[2,3], (Member, IEEE)
[1]Institute of Physics, École Polytechnique Fédérale de Lausanne (EPFL), CH-1015 Lausanne, Switzerland
[2]School of Engineering, University of Applied Sciences of Western Switzerland, HES-SO CH-1951 Sierre, Switzerland
[3]Department of Quantum Matter Physics, University of Geneva, CH-1211 Geneva, Switzerland

Corresponding author: Laurent Pagnier (laurent.vincent.pagnier@gmail.com)

This work was supported by the Swiss National Science Foundation under Grant PYAPP2_154275 and Grant 200020_182050.

ABSTRACT The increasing penetration of new renewable sources of electrical energy reduces the overall mechanical inertia available in power grids. This raises a number of issues regarding grid stability over short to medium time scales. A number of approaches have been proposed to compensate for this inertia reduction by deploying substitution inertia in the form of synchronous condensers, flywheels or power-electronic-based synthetic inertia. These resources are limited and expensive; therefore, a key issue is to determine how to optimally place them in the power grid, for instance, to mitigate voltage angle and frequency disturbances following an abrupt power loss. Performance measures in the form of $\mathcal{H}_2-$norms have recently been introduced to evaluate the overall magnitude of such disturbances. However, despite the mathematical convenience of these measures, analytical results can only be obtained under rather unrealistic assumptions of a uniform damping-to-inertia ratio or a homogeneous distribution of the inertia and/or primary control. Here, we introduce and apply matrix perturbation theory to obtain analytical results for an optimal inertia and primary control placement in the case where both are heterogeneous. This powerful method allows us to construct two simple algorithms that independently optimize the geographical distribution of the inertia and primary control. The algorithms are then implemented for a numerical model of the synchronous transmission grid of continental Europe with different initial configurations. We find that an inertia redistribution has little effect on the grid performance but that the primary control should be redistributed on the slow modes of the network, where the intrinsic grid dynamic requires more time to damp frequency disturbances. For a budget-constraint optimization, we show that increasing the amount of primary control in the periphery of the grid, without changing the inertia distribution, achieves 90 % or more of the maximal possible optimization, already for relatively moderate budgets.

INDEX TERMS Low-inertia transmission grids, optimal placement of inertia and primary control, perturbation theory.

I. INTRODUCTION

The penetration of new renewable energy sources (RESs), such as photovoltaic panels and wind turbines, is increasing in most electric power grids worldwide. Currently, these energy sources are connected to power grids via inverters, which make them essentially inertialess. Accordingly, the increased penetration leads to periods of unusually low inertia at times of high-RES production [1]. This raises important issues regarding the power grid stability, which is of more concern to transmission system operators than the volatility of RES production [2], [3]. The substitution of traditional production based on synchronous machines with inertialess RES may in particular lead to geographically inhomogeneous inertia profiles. It has been suggested to deploy substitution inertia – synthetic inertia, flywheels or synchronous condensers – to compensate locally or globally for the missing inertia. Two related questions naturally arise: (i) where is it safe to substitute synchronous machines with inertialess RES, and (ii) where is it necessary to accompany the deployment of

The associate editor coordinating the review of this manuscript and approving it for publication was Siqi Bu.

new RES with substitution inertia? Problem (ii) has been investigated in small power grid models with up to a dozen buses, optimizing the geographical distribution of the inertia against cost functions based on eigenvalue damping ratios [4], $\mathcal{H}_p$-norms [5], [6] and RoCoF [7], [8] and frequency excursions [8]. Investigations of problem (i) in large power grids have emphasized the importance of the geographical extent of the slow network modes [9]. A numerical optimization can certainly be performed for any given network on a case-by-case basis; however, it is highly desirable to shed light on the problem with analytical results. So far, such results have either been restricted to small systems or derived assuming homogeneity in the damping and inertia parameters or their ratio. In this manuscript, we go beyond these assumptions and construct an approach that is applicable to realistic large power grids with inhomogeneous independent damping and inertia parameters.

Inspired by theoretical physics, we introduce *matrix perturbation theory* [10] as an analytical tool to tackle this problem. That method is widely used in quantum mechanics to approximate solutions to complex, perturbed problems, extrapolated from known, exact solutions of integrable problems [11]. Matrix perturbation theory is a spectral method that allows the expression of eigenvalues and eigenvectors of the matrix corresponding to the full, complex problem in a controlled series about the eigenvalues and eigenvectors of a simpler, exactly solvable problem. The approximation is useful as long as the two problems are not too different and it makes sense to consider the full, complex problem as a *perturbation* of the exactly soluble, simpler problem. When this is the case, the perturbation expansion converges rapidly, and its truncation at low orders delivers rather accurate results. In the context of electric power grids, this method was applied, for instance, in Ref. [12], where quadratic performance measures similar to those discussed below were calculated following a line fault, starting from the eigenvalues and eigenvectors of the network Laplacian before the fault.

In this paper, we consider abrupt power losses in high-voltage electric power grids. We aim to determine the best geographical distribution of inertia and primary control to mitigate the ensuing transient excursion. To do so, we apply matrix perturbation theory [10] to evaluate the magnitude of the transient excursion in a series expansion to first order in the inertia and primary control inhomogeneities. Our perturbation theory is an expansion in two parameters: the maximal deviations δm and δd of the rotational inertia and the damping parameters from their initial values m and d. The approach is valid as long as these local deviations are small; i.e., $|\delta m/m| < 1$, $|\delta d/d| < 1$. In principle, these conditions tolerate that inertia and damping parameters vanish or are twice as large as their average values in some buses. The theory constructed below constitutes an important step forward in the analytical optimization of inertia and primary control placement in low-inertia power grids. In fact, the approach allows us to to derive analytical results without relying on homogeneity assumptions regarding the inertia and primary control or assuming that their ratios are constant. To the best of our knowledge, earlier analytical works have all been based on such mathematically convenient but unrealistic assumptions. Our main analytical results are given in Theorems 1 and 2 below, which formulate the algorithms for the optimal placement of the local inertia and damping parameters. The spectral decomposition approach used here has recently drawn the attention of a number of groups and has been used to calculate performance measures in power grids and consensus algorithms, e.g., in [7], [13]–[15]. This paper builds up on our earlier work [16].

The article is organized as follows. Section II addresses the case where the inertia and primary control are uniformly distributed in the system. The performance measure that quantifies the system disturbances is introduced, and we calculate its value for abrupt power losses. In Section III, we apply matrix perturbation theory to calculate the sensitivities of our measure for local variations in the inertia and primary control. Section IV presents our analytical theory for the optimal placement of inertia and primary control. In Section V, we apply our optimal placements to a model of the continental European grid. Three different initial configurations are considered, for which budget-constraint optimizations are performed. Section VI concludes our article.

II. HOMOGENEOUS CASE

We consider the power system dynamics in the lossless line approximation, which is a standard approximation used for high-voltage transmission grids [17]. On time scales ranging from a few AC cycles to approximately 10-20 seconds, the transient dynamics are governed by the swing equations [17]:

$$m_i\dot{\omega}_i + d_i\omega_i = P_i - \sum_j B_{ij}\sin(\theta_i - \theta_j)\,. \tag{1}$$

This set of differential equations gives the dynamics of the voltage angles θ_i and frequencies $\omega_i = \dot{\theta}_i$ at each network bus labeled $i = 1,\dots N$ in a frame rotating at the rated grid frequency of 50 or 60 Hz. Each bus is characterized by inertia, m_i, and damping/primary control, d_i, parameters, and P_i is the active power injected ($P_i > 0$) or extracted ($P_i < 0$) at bus i. We introduce the damping-to-inertia ratio $\gamma_i \equiv d_i/m_i$. The buses are connected to each other via lines with susceptances B_{ij}. The operating state is given by stationary solutions $\{\theta_i^{(0)}\}$ to (1), i.e., power flow solutions determined by $P_i = \sum_j B_{ij}\sin(\theta_i^{(0)} - \theta_j^{(0)})$. The small-signal response about such a solution under a change in active power $P_i \to P_i + \delta P_i$ is obtained by linearizing (1) about such a solution with $\theta_i(t) = \theta_i^{(0)} + \delta\theta_i(t)$. One has, in matrix form,

$$\boldsymbol{M}\dot{\boldsymbol{\omega}} + \boldsymbol{D}\boldsymbol{\omega} = \boldsymbol{\delta P} - \boldsymbol{L}\boldsymbol{\delta\theta}\,, \tag{2}$$

where $\boldsymbol{M} = \mathrm{diag}(\{m_i\})$, $\boldsymbol{D} = \mathrm{diag}(\{d_i\})$ and the voltage angles and frequencies are cast into vectors $\boldsymbol{\delta\theta}$ and $\boldsymbol{\omega} \equiv \boldsymbol{\delta\dot{\theta}}$. The Laplacian matrix $\boldsymbol{L}$ has matrix elements $L_{ij} = -B_{ij}\cos(\theta_i^{(0)} - \theta_j^{(0)})$, for $i \neq j$, and $L_{ii} = \sum_k B_{ik}\cos(\theta_i^{(0)} - \theta_k^{(0)})$.

A. EXACT SOLUTION FOR THE HOMOGENEOUS DAMPING-TO-INERTIA RATIO

When the damping-to-inertia ratio is constant, $d_i/m_i = \gamma_i = \gamma, \forall i$, (2) can be integrated exactly [7], [12]. To see this, we first transform the angle coordinates as $\boldsymbol{\delta\theta} = \boldsymbol{M}^{-1/2}\boldsymbol{\delta\theta_M}$ to obtain

$$\dot{\boldsymbol{\omega}}_M + \underbrace{\boldsymbol{M}^{-1}\boldsymbol{D}}_{\boldsymbol{\Gamma}}\boldsymbol{\omega}_M + \underbrace{\boldsymbol{M}^{-1/2}\boldsymbol{L}\boldsymbol{M}^{-1/2}}_{\boldsymbol{L_M}}\boldsymbol{\delta\theta}_M = \boldsymbol{M}^{-1/2}\boldsymbol{\delta P}\,, \tag{3}$$

where we have introduced the diagonal matrix $\boldsymbol{\Gamma} = \mathrm{diag}(\{d_i/m_i\}) \equiv \mathrm{diag}(\{\gamma\})$. The change of coordinates substitutes the Laplacian matrix $\boldsymbol{L}$ with a matrix $\boldsymbol{L_M}$ that is weighted by inertia. Since the matrix is real and symmetric, $\boldsymbol{L_M}$ can be diagonalized

$$\boldsymbol{L_M} = \boldsymbol{U}^\top\boldsymbol{\Lambda}\boldsymbol{U} \tag{4}$$

with an orthogonal matrix $\boldsymbol{U}$, and the α^{th} row of this matrix gives the components $u_{\alpha,i}$, $i = 1,\dots N$ of the α^{th} eigenvector $\boldsymbol{u}_\alpha$ of $\boldsymbol{L_M}$. The diagonal matrix $\boldsymbol{\Lambda} = \mathrm{diag}(\{\lambda_1 = 0, \lambda_2, \cdots, \lambda_N\})$ contains the eigenvalues of $\boldsymbol{L_M}$ in increasing order $\lambda_\alpha < \lambda_{\alpha+1}$. For stable networks, the smallest eigenvalue λ_1 vanishes, corresponding to the eigenvector with components $u_{1i} = \sqrt{m_i}/\sqrt{\sum_j m_j}$. If the network is connected, it is the only vanishing eigenvalue. Rewriting (3) in the basis diagonalizing $\boldsymbol{L_M}$ gives

$$\ddot{\boldsymbol{\xi}} + \boldsymbol{U}\boldsymbol{\Gamma}\boldsymbol{U}^\top\dot{\boldsymbol{\xi}} + \boldsymbol{\Lambda}\boldsymbol{\xi} = \boldsymbol{U}\boldsymbol{M}^{-1/2}\boldsymbol{\delta P}\,, \tag{5}$$

where $\boldsymbol{\delta\theta_M} = \boldsymbol{U}^\top\boldsymbol{\xi}$. This change of coordinates is simply a spectral decomposition of the angle deviations $\boldsymbol{\delta\theta_M}$ into their components in the basis of the eigenvectors of $\boldsymbol{L_M}$. These components are cast in the vector $\boldsymbol{\xi}$. The formulation (5) of the problem makes it clear that, if $\boldsymbol{\Gamma}$ is a multiple of the identity matrix, the problem reduces to an exactly integrable diagonal ordinary differential equation problem. This case is treated below in (11), which provides an exact solution about which we then construct the matrix perturbation theory.

Proposition 1 (Unperturbed evolution): For an abrupt power loss, $\boldsymbol{\delta P}(t) = \boldsymbol{\delta P}\,\Theta(t)$, with the Heaviside step function defined by $\Theta(t > 0) = 1$ and $\Theta(t < 0) = 0$ and with a homogeneous damping-to-inertia ratio, $\boldsymbol{\Gamma} = \gamma\,\mathbb{1}$ with the $N \times N$ identity matrix $\mathbb{1}$, the frequency coordinates $\dot{\xi}_\alpha$ evolve independently as

$$\dot{\xi}_\alpha(t) = \frac{2\mathcal{P}_\alpha}{f_\alpha}e^{-\gamma t/2}\sin\left(\frac{f_\alpha t}{2}\right), \quad \forall\alpha > 1, \tag{6}$$

where $f_\alpha = \sqrt{4\lambda_\alpha - \gamma^2}$ and $\mathcal{P}_\alpha = \sum_i u_{\alpha i}\,\delta P_i/m_i^{1/2}$.

This result generalizes Theorem III.3 of [14].

Proof: The proof follows the procedure proposed in [7], [12], [18]. First, one rewrites (5) as

$$\frac{\mathrm{d}}{\mathrm{d}t}\begin{bmatrix}\boldsymbol{\xi}\\ \dot{\boldsymbol{\xi}}\end{bmatrix} = \underbrace{\begin{bmatrix}\mathbb{0}_{N\times N} & \mathbb{1}\\ -\boldsymbol{\Lambda} & -\gamma\,\mathbb{1}\end{bmatrix}}_{\boldsymbol{H}_0}\begin{bmatrix}\boldsymbol{\xi}\\ \dot{\boldsymbol{\xi}}\end{bmatrix} + \begin{bmatrix}\mathbb{0}_{N\times 1}\\ \boldsymbol{\mathcal{P}}\end{bmatrix}, \tag{7}$$

where $\boldsymbol{\mathcal{P}} = \boldsymbol{U}\boldsymbol{M}^{-1/2}\boldsymbol{\delta P}$ and $\mathbb{0}_{N\times M}$ is an $N \times M$ matrix of zeroes. The matrix $\boldsymbol{H}_0$ is block-diagonal up to a permutation of rows and columns [12], with each 2×2 block corresponding to one of the eigenvalues λ_α of $\boldsymbol{L_M}$. The α^{th} block is easily diagonalized by the transformation

$$\begin{bmatrix}\chi^{(0)}_{\alpha+}\\ \chi^{(0)}_{\alpha-}\end{bmatrix} = \boldsymbol{T}^L_\alpha\begin{bmatrix}\xi_\alpha\\ \dot{\xi}_\alpha\end{bmatrix}, \quad \boldsymbol{T}^L_\alpha \equiv \frac{i}{f_\alpha}\begin{bmatrix}\mu^{(0)}_{\alpha-} & -1\\ -\mu^{(0)}_{\alpha+} & 1\end{bmatrix}, \tag{8}$$

$$\begin{bmatrix}\xi_\alpha\\ \dot{\xi}_\alpha\end{bmatrix} = \boldsymbol{T}^R_\alpha\begin{bmatrix}\chi^{(0)}_{\alpha+}\\ \chi^{(0)}_{\alpha-}\end{bmatrix}, \quad \boldsymbol{T}^R_\alpha \equiv \begin{bmatrix}1 & 1\\ \mu^{(0)}_{\alpha+} & \mu^{(0)}_{\alpha-}\end{bmatrix}, \tag{9}$$

with the eigenvalues $\mu^{(0)}_{\alpha\pm}$ of the α^{th} block,

$$\mu^{(0)}_{\alpha\pm} = -\frac{1}{2}(\gamma \mp i f_\alpha)\,. \tag{10}$$

The two rows (columns) of $\boldsymbol{T}^L_\alpha$ ($\boldsymbol{T}^R_\alpha$) provide the nonzero components of the two left (right) eigenvectors $\boldsymbol{t}^{(0)L}_{\alpha\pm}$ ($\boldsymbol{t}^{(0)R}_{\alpha\pm}$) of $\boldsymbol{H}_0$. Following this transformation, (7) is

$$\frac{\mathrm{d}}{\mathrm{d}t}\begin{bmatrix}\chi^{(0)}_{\alpha+}\\ \chi^{(0)}_{\alpha-}\end{bmatrix} = \begin{bmatrix}\mu^{(0)}_{\alpha+} & 0\\ 0 & \mu^{(0)}_{\alpha-}\end{bmatrix}\begin{bmatrix}\chi^{(0)}_{\alpha+}\\ \chi^{(0)}_{\alpha-}\end{bmatrix} + \frac{i}{f_\alpha}\begin{bmatrix}-\mathcal{P}_\alpha\\ \mathcal{P}_\alpha\end{bmatrix}. \tag{11}$$

With the initial condition $\xi_\alpha(t = 0) = \dot{\xi}_\alpha(t = 0) = 0$, which implies that $\chi^{(0)}_{\alpha\pm}(t = 0) = 0$, (11) is easily integrated, leading to

$$\chi^{(0)}_{\alpha\pm} = \pm\tfrac{i\mathcal{P}_\alpha}{f_\alpha\mu^{(0)}_{\alpha\pm}}\left(1 - e^{\mu^{(0)}_{\alpha\pm}t}\right), \quad \forall\alpha > 1\,. \tag{12}$$

Equation (6) is finally obtained by inserting (12) into (8), which concludes the proof. ∎

B. PERFORMANCE MEASURE

We wish to mitigate disturbances following an abrupt power loss. To this end, we use performance measures that evaluate the overall disturbance magnitude over time and the whole power grid. Performance measures have been proposed that can be formulated as $\mathcal{L}_2$- and squared $\mathcal{H}_2$-norms of linear systems [6], [7], [12], [18]–[24] and are time-integrated quadratic forms of the angle, $\boldsymbol{\delta\theta}$, or frequency, $\boldsymbol{\omega}$, deviations. Here, we focus on frequency deviations and use the following performance measure:

$$\mathcal{M} = \int_0^\infty (\boldsymbol{\omega}^\top - \bar{\boldsymbol{\omega}}^\top)\boldsymbol{M}(\boldsymbol{\omega} - \bar{\boldsymbol{\omega}})\mathrm{d}t\,, \tag{13}$$

where $\bar{\boldsymbol{\omega}} = (\omega_{\text{sys}}, \omega_{\text{sys}}, \dots \omega_{\text{sys}})^\top$ is the instantaneous average frequency vector with components

$$\omega_{\text{sys}}(t) = \sum_i m_i\omega_i(t)\Big/\sum_i m_i\,. \tag{14}$$

Rewriting $\mathcal{M}$ in the eigenbasis of $\boldsymbol{L_M}$ gives

$$\mathcal{M} = \int_0^\infty \sum_{\alpha>1}\dot{\xi}^2_\alpha(t)\mathrm{d}t\,, \tag{15}$$

since the first eigenvector of $\boldsymbol{L_M}$ (with a zero eigenvalue) has components $u_{1i} = \sqrt{m_i}/\sqrt{\sum_j m_j}$.

Proposition 2: For an abrupt power loss, $\boldsymbol{\delta P}(t) = \boldsymbol{\delta P}\,\Theta(t)$, on a single bus labeled b with a homogeneous

damping-to-inertia ratio $\mathbf{\Gamma} = \gamma\,\mathbb{1}$ *with the* $N \times N$ *identity matrix* $\mathbb{1}$*, the performance measure* (13) *is*

$$\mathcal{M}_b = \frac{\delta P^2}{2\gamma m_b} \sum_{\alpha>1} \frac{u_{\alpha b}^2}{\lambda_\alpha}\,, \tag{16}$$

in terms of the eigenvalues λ_α *and the components* $u_{\alpha b}$ *of the eigenvectors* $\boldsymbol{u}_\alpha$ *of* $\boldsymbol{L_M}$.

Note that we introduce the subscript b to indicate that the fault is localized on that bus only. The power loss is modeled as $P_i = P_i^{(0)} - \delta P_i\,\Theta(t)$ with $\delta P_i = \delta_{ib}\,\delta P$, where the Kronecker symbol is $\delta_{ib} = 1$ if $i = b$ and 0 otherwise.

Proof: (6) straightforwardly gives

$$\int_0^\infty \dot{\xi}_\alpha^2(t)\mathrm{d}t = \frac{\delta P^2\, u_{\alpha b}^2}{2\gamma\, m_b\, \lambda_\alpha}\,, \quad \alpha > 1\,, \tag{17}$$

which, when summed over $\alpha > 1$, gives (16). ∎

Remark 1: For the homogeneous inertia coefficients, $\boldsymbol{M} = m\mathbb{1}$*, the eigenvectors and eigenvalues of the inertia-weighted matrix* $\boldsymbol{L_M}$ *defined in* (3) *are given by* $\boldsymbol{u}_\alpha = \boldsymbol{u}_\alpha^{(0)}$ *and* $\lambda_\alpha = m^{-1}\lambda_\alpha^{(0)}$ *in terms of the eigenvectors* $\boldsymbol{u}_\alpha^{(0)}$ *and eigenvalues* $\lambda_\alpha^{(0)}$ *of the Laplacian* $\boldsymbol{L}$*. In this case, the performance measure is*

$$\mathcal{M}_b^{(0)} = \frac{\delta P^2}{2\gamma} \sum_{\alpha>1} \frac{u_{\alpha b}^{(0)2}}{\lambda_\alpha^{(0)}}\,. \tag{18}$$

Here the superscript $^{(0)}$ *indicates inertia homogeneity. This expression has an interesting graph theoretic interpretation. We recall the definitions of the resistance distance* Ω_{ij} *between two nodes on the network, the associated centrality* C_j *and the generalized Kirchhoff indices* Kf_p *[23], [25],*

$$\Omega_{ij} = \boldsymbol{L}_{ii}^\dagger + \boldsymbol{L}_{jj}^\dagger - \boldsymbol{L}_{ij}^\dagger - \boldsymbol{L}_{ji}^\dagger\,, \tag{19}$$

$$C_j = N\left(\sum_i \Omega_{ij}\right)^{-1}\,, \tag{20}$$

$$Kf_p = N\sum_{\alpha>1} \lambda_\alpha^{-p}\,, \tag{21}$$

where $\boldsymbol{L}^\dagger$ *is the Moore–Penrose pseudoinverse of* $\boldsymbol{L}$*. With these definitions, one can show that [15], [23], [26]*

$$\sum_{\alpha>1} \frac{u_{\alpha b}^{(0)2}}{\lambda_\alpha^{(0)}} = C_b^{-1} - N^{-2} Kf_1\,, \tag{22}$$

using the spectral representation of the resistance distance [27], [28]

$$\Omega_{ib} = \sum_{\alpha>1} \left(u_{\alpha i}^{(0)} - u_{\alpha b}^{(0)}\right)^2 / \lambda_\alpha^{(0)}\,. \tag{23}$$

Because Kf_1 *is a global quantity characterizing the network, it follows from* (18) *with* (22) *that, when the inertia and primary control are homogeneously distributed in the system, the disturbance magnitude as measured by* $\mathcal{M}_b^{(0)}$ *is larger for disturbances on peripheral nodes [9], [29].*

III. MATRIX PERTURBATION

The previous section treats the case where the inertia and primary control are uniformly distributed in the system. Our goal is to lift this restriction and obtain $\mathcal{M}_b$ when some mild inhomogeneities are present. We parametrize the inhomogeneities in the inertia and damping-to-inertia ratio as

$$m_i = m + \delta m\, r_i\,, \tag{24}$$

$$d_i = m_i\gamma_i = (m + \delta m\, r_i)(\gamma + \delta\gamma\, a_i)\,, \tag{25}$$

in terms of the averages m and γ and the maximum amplitude of the deviations δm and $\delta\gamma$ (which we will call "inhomogeneity parameters"). Local inhomogeneities are determined by the coefficients $-1 \le a_i, r_i \le 1$ with $\sum_i r_i = \sum_i a_i = 0$, which are determined following a minimization of the performance measure $\mathcal{M}_b$ of (13). In the following two paragraphs, we construct the matrix perturbation theory to first order in δm and $\delta\gamma$ to calculate the performance measure $\mathcal{M}_b = \mathcal{M}_b^{(0)} + \sum_i r_i\rho_i + \sum_i a_i\alpha_i + \mathcal{O}(\delta m^2, \delta\gamma^2)$. This requires a calculation of the susceptibilities $\rho_i \equiv \partial\mathcal{M}_b/\partial r_i$ and $\alpha_i \equiv \partial\mathcal{M}_b/\partial a_i$.

A. INHOMOGENEITY IN THE INERTIA

When the inertia is inhomogeneous but the damping-to-inertia ratio is homogeneous, the system dynamics and $\mathcal{M}_b$ are still given by (7) and (16). However, the eigenvectors of the inertia-weighted Laplacian matrix $\boldsymbol{L_M}$ differ from those of $\boldsymbol{L}$, and consequently $\mathcal{M}_b$ is no longer equal to $\mathcal{M}_b^{(0)}$. In general, there is no simple way to diagonalize $\boldsymbol{L_M}$; however, one expects that if the inhomogeneity is weak, then the eigenvalues and eigenvectors of $\boldsymbol{L_M}$ will only slightly differ from those of $m^{-1}\boldsymbol{L}$, which allows the construction of a perturbation theory.

Assumption 1 (Weak inhomogeneity in the inertia): The deviations $\delta m\, r_i$ *of the local inertia* m_i *are all small compared to their average* m*. We write* $\boldsymbol{M} = m\big[\mathbb{1} + \mu\,\mathrm{diag}(\{r_i\})\big]$*, where* $\mu \equiv \delta m/m \ll 1$ *is a small, dimensionless parameter.*

To linear order in μ, the series expansion of $\boldsymbol{L_M}$ is

$$\boldsymbol{L_M} = \boldsymbol{M}^{-1/2}\boldsymbol{L}\boldsymbol{M}^{-1/2} = m^{-1}\big[\boldsymbol{L} + \mu\boldsymbol{V}_1 + \mathcal{O}(\mu^2)\big]\,, \tag{26}$$

with $\boldsymbol{V}_1 = -\big(\boldsymbol{R}\boldsymbol{L} + \boldsymbol{L}\boldsymbol{R}\big)/2$ and $\boldsymbol{R} = \mathrm{diag}(\{r_i\})$. In this form, the inertia-weighted Laplacian matrix $\boldsymbol{L_M}$ is given by the sum of an easily diagonalizable matrix, $m^{-1}\boldsymbol{L}$, and a small perturbation matrix, $(\mu/m)\,\boldsymbol{V}_1$. Truncating the expansion of $\boldsymbol{L_M}$ at this linear order gives an error of order $\sim \mu^2$, which is small under Assumption 1.

Matrix perturbation theory expands the eigenvectors $\boldsymbol{u}_\alpha$ and eigenvalues λ_α of the full problem $\boldsymbol{L_M}$ in a power series in μ depending on the eigenvectors ($\boldsymbol{u}_\alpha^{(0)}$ and eigenvalues $\lambda_\alpha^{(0)}$) of $\boldsymbol{L}$ [10]. To first order in μ, one has

$$\lambda_\alpha = m^{-1}\big[\lambda_\alpha^{(0)} + \mu\lambda_\alpha^{(1)} + \mathcal{O}(\mu^2)\big]\,, \tag{27}$$

$$\boldsymbol{u}_\alpha = \boldsymbol{u}_\alpha^{(0)} + \mu\boldsymbol{u}_\alpha^{(1)} + \mathcal{O}(\mu^2)\,, \tag{28}$$

with

$$\lambda_\alpha^{(1)} = \boldsymbol{u}_\alpha^{(0)\top}\boldsymbol{V}_1\boldsymbol{u}_\alpha^{(0)}\,, \tag{29}$$

$$\boldsymbol{u}_\alpha^{(1)} = \sum_{\beta\neq\alpha} \frac{\boldsymbol{u}_\beta^{(0)\top} \boldsymbol{V}_1 \boldsymbol{u}_\alpha^{(0)}}{\lambda_\alpha^{(0)} - \lambda_\beta^{(0)}} \boldsymbol{u}_\beta^{(0)} \,. \tag{30}$$

From (16), (27) and (28), the performance measure $\mathcal{M}_b$ can be approximated to first order in μ as

$$\mathcal{M}_b = \mathcal{M}_b^{(0)} + \frac{\mu\delta P^2}{2\gamma} \sum_{\alpha>1} \lambda_\alpha^{(0)-1} \Big(2u_{\alpha b}^{(0)} u_{\alpha b}^{(1)} - r_b u_{\alpha b}^{(0)2} - u_{\alpha b}^{(0)2} \lambda_\alpha^{(0)-1} \lambda_\alpha^{(1)} \Big) + \mathcal{O}(\mu^2) \,. \tag{31}$$

Proposition 3: For an abrupt power loss, $\boldsymbol{\delta P}(t) = \boldsymbol{\delta P}\,\Theta(t)$, on a single bus labeled b, where $\delta P_i = \delta_{ib}\,\delta P$, and under Assumption 1, the susceptibilities $\rho_i \equiv \partial\mathcal{M}_b/\partial r_i$ are given by

$$\rho_i = -\frac{\mu\delta P^2}{\gamma N} \sum_{\alpha>1} \frac{u_{\alpha b}^{(0)} u_{\alpha i}^{(0)}}{\lambda_\alpha^{(0)}} \,. \tag{32}$$

Proof: We first take the derivative of (31) with respect to r_i, with $\lambda_\alpha^{(1)}$ and $u_{\alpha b}^{(1)}$ from (29) and (30). We obtain

$$\frac{\partial\mathcal{M}_b}{\partial r_i} = \frac{\mu\delta P^2}{2\gamma} \Bigg[\sum_{\substack{\alpha>1,\\ \beta\neq\alpha}} u_{\alpha b}^{(0)} u_{\beta b}^{(0)} u_{\alpha i}^{(0)} u_{\beta i}^{(0)} \left(\frac{1}{\lambda_\alpha^{(0)}} - \frac{2}{\lambda_\alpha^{(0)} - \lambda_\beta^{(0)}} \right) - \delta_{ib} \sum_{\alpha>1} \frac{u_{\alpha b}^{(0)2}}{\lambda_\alpha^{(0)}} + \sum_{\alpha>1} \frac{u_{\alpha b}^{(0)2} u_{\alpha i}^{(0)2}}{\lambda_\alpha^{(0)}} \Bigg] + \mathcal{O}(\mu^2) \,, \tag{33}$$

The first term in the square bracket in (33) gives

$$\sum_{\substack{\alpha>1\\ \beta\neq\alpha}} \frac{u_{\alpha b}^{(0)} u_{\beta b}^{(0)} u_{\alpha i}^{(0)} u_{\beta i}^{(0)}}{\lambda_\alpha^{(0)}} = \sum_{\substack{\alpha>1,\\ \beta}} \frac{u_{\alpha b}^{(0)} u_{\beta b}^{(0)} u_{\alpha i}^{(0)} u_{\beta i}^{(0)}}{\lambda_\alpha^{(0)}} - \sum_{\alpha>1} \frac{u_{\alpha b}^{(0)2} u_{\alpha i}^{(0)2}}{\lambda_\alpha^{(0)}} = \delta_{ib} \sum_{\alpha>1} \frac{u_{\alpha b}^{(0)2}}{\lambda_\alpha^{(0)}} - \sum_{\alpha>1} \frac{u_{\alpha b}^{(0)2} u_{\alpha i}^{(0)2}}{\lambda_\alpha^{(0)}} \,, \tag{34}$$

where we used $\sum_\beta u_{\beta i}^{(0)} u_{\beta b}^{(0)} = \delta_{ib}$. This term therefore exactly cancels the last two terms in the square bracket in (33), and one obtains

$$\rho_i(b) = \frac{\partial\mathcal{M}_b}{\partial r_i} = -\frac{\mu\delta P^2}{\gamma} \sum_{\substack{\alpha>1,\\ \beta\neq\alpha}} \frac{u_{\alpha b}^{(0)} u_{\beta b}^{(0)} u_{\alpha i}^{(0)} u_{\beta i}^{(0)}}{\lambda_\alpha^{(0)} - \lambda_\beta^{(0)}} + \mathcal{O}(\mu^2) \,. \tag{35}$$

The argument of the double sum in (35) is odd under a permutation of α and β; therefore, the only terms that do not vanish are those with $\beta = 1$. With $u_{1i}^{(0)} = 1/\sqrt{N}$, one finally obtains (32). ∎

Remark 2: The sum of the susceptibilities over all possible fault locations vanishes: $\sum_b \rho_i(b) = 0$. This follows from the properties of the eigenvector $\boldsymbol{u}_\alpha^{(0)}$, $\alpha > 1$.

B. INHOMOGENEITY IN THE DAMPING-TO-INERTIA RATIO

Equation (6) gives exact solutions to the linearized dynamical problem defined in (5) under the assumption of a homogeneous damping-to-inertia ratio, $d_i/m_i \equiv \gamma$. Next, we go beyond this assumption and allow for homogeneities in the damping-to-inertia ratio. We write $\gamma_i = \gamma + \delta\gamma\, a_i$. With these inhomogeneities, (7) is

$$\frac{\mathrm{d}}{\mathrm{d}t} \begin{bmatrix} \boldsymbol{\xi} \\ \dot{\boldsymbol{\xi}} \end{bmatrix} = \underbrace{\begin{bmatrix} \mathbb{0}_{N\times N} & \mathbb{1} \\ -\boldsymbol{\Lambda} & -\gamma\,\mathbb{1} - \delta\gamma\,\boldsymbol{V}_2 \end{bmatrix}}_{\boldsymbol{H}} \begin{bmatrix} \boldsymbol{\xi} \\ \dot{\boldsymbol{\xi}} \end{bmatrix} + \begin{bmatrix} \mathbb{0}_{N\times 1} \\ \boldsymbol{\mathcal{P}} \end{bmatrix}, \tag{36}$$

which differs from (7) only through the additional term $-\delta\gamma\boldsymbol{V}_2$, where $\boldsymbol{V}_2 = \boldsymbol{U}\boldsymbol{A}\,\boldsymbol{U}^\top$ and $\boldsymbol{A} = \mathrm{diag}(\{a_i\})$. Under the assumption that $g \equiv \delta\gamma/\gamma \ll 1$, this additional term only introduces small corrections to the unperturbed problem of (7), and we use matrix perturbation theory to calculate these corrections in a polynomial expansion in g.

Assumption 2 (Weak inhomogeneity in the damping-to-inertia ratio): The deviations $\delta\gamma\, a_i$ of the damping-to-inertia ratio γ_i from the average γ are all small compared to the average. We write $\boldsymbol{\Gamma} = \gamma\big[\mathbb{1} + g\,\mathrm{diag}\big(\{a_i\}\big)\big]$, where $g \equiv \delta\gamma/\gamma \ll 1$ is a small, dimensionless parameter.

Our goal is to integrate (36) using the spectral approach used above to derive (12). This requires exactly knowing the eigenvalues and eigenvectors of $\boldsymbol{H}$ in (36); however, this is not possible in general, because the matrices $\boldsymbol{V}_2$ and $\boldsymbol{\Lambda}$ do not commute. As long as g is sufficiently small, the eigenvalues and eigenvectors are only slightly altered [10] and can be systematically calculated order by order in a polynomial expansion in g. Therefore, we employ a perturbative approach that expresses the solutions to (36) in a polynomial expansion in g. Formally, for the eigenvalues $\mu_{\alpha s}$ and the left and right eigenvectors $\boldsymbol{t}_{\alpha s}^{L,R}$ of $\boldsymbol{H}$, one has

$$\mu_{\alpha s} = \sum_{m=0}^{\infty} g^m\, \mu_{\alpha s}^{(m)} \,, \tag{37}$$

$$\boldsymbol{t}_{\alpha s}^{L,R} = \sum_{m=0}^{\infty} g^m\, \boldsymbol{t}_{\alpha s}^{(m)L,R} \,, \tag{38}$$

where the $m = 0$ terms are given by the eigenvalues $\mu_{\alpha s}^{(0)}$ and the left and right eigenvectors $\boldsymbol{t}_{\alpha s}^{(0)L,R}$ of the matrix $\boldsymbol{H}_0$ in (7), corresponding to homogeneous inertia. For the sums in (37) and (38) to converge, a necessary condition is that $g < 1$. Then, the task is to calculate the terms $\mu_{\alpha s}^{(m)}$ and $\boldsymbol{t}_{\alpha s}^{(m)L,R}$ with $m = 1, 2, \ldots$. When $g \ll 1$, one expects that only a few low-order terms will provide a good estimate of the eigenvalues and eigenvectors of $\boldsymbol{H}$. Here, we calculate the first-order corrections, with $m = 1$. The corrections are given by formulas similar to (29) and (30):

$$g\,\mu_{\alpha s}^{(1)} = \boldsymbol{t}_{\alpha s}^{(0)L} \begin{bmatrix} \mathbb{0}_{N\times N} & \mathbb{0}_{N\times N} \\ \mathbb{0}_{N\times N} & -\delta\gamma\,\boldsymbol{V}_2 \end{bmatrix} \boldsymbol{t}_{\alpha s}^{(0)R} \,, \tag{39}$$

$$g\,\boldsymbol{t}_{\alpha s}^{(1)R} = \sum_{\beta,s'}{}' \frac{\boldsymbol{t}_{\beta s'}^{(0)L} \begin{bmatrix} \mathbb{0}_{N\times N} & \mathbb{0}_{N\times N} \\ \mathbb{0}_{N\times N} & -\delta\gamma\,\boldsymbol{V}_2 \end{bmatrix} \boldsymbol{t}_{\alpha s}^{(0)R}}{\mu_{\alpha s}^{(0)} - \mu_{\beta s'}^{(0)}} \boldsymbol{t}_{\beta s'}^{(0)R} \,, \tag{40}$$

$$g\,\boldsymbol{t}_{\alpha s}^{(1)L} = \sum_{\beta,s'}{}' \frac{\boldsymbol{t}_{\alpha s}^{(0)L} \begin{bmatrix} \mathbb{0}_{N\times N} & \mathbb{0}_{N\times N} \\ \mathbb{0}_{N\times N} & -\delta\gamma\,\boldsymbol{V}_2 \end{bmatrix} \boldsymbol{t}_{\beta s'}^{(0)R}}{\mu_{\alpha s}^{(0)} - \mu_{\beta s'}^{(0)}} \boldsymbol{t}_{\beta s'}^{(0)L} \,, \tag{41}$$

where $\overline{\sum}$ indicates that the sum is taken over $(\beta, s') \neq (\alpha, s)$. One obtains

$$g\,\mu_{\alpha s}^{(1)} = -\delta\gamma\Big(\frac{1}{2} + is\frac{\gamma}{2f_\alpha}\Big)\boldsymbol{V}_{2;\alpha\alpha}\,, \tag{42}$$

$$g\,\boldsymbol{t}_{\alpha s}^{(1)R} = 2\,\delta\gamma\,\overline{\sum_{\beta,s'}}\frac{\boldsymbol{V}_{2;\alpha\beta}\,\mu_{\alpha s}^{(0)}}{f_\beta(ss'f_\alpha - f_\beta)}\,\boldsymbol{t}_{\beta s'}^{(0)R}\,, \tag{43}$$

$$g\,\boldsymbol{t}_{\alpha s}^{(1)L} = 2\,\delta\gamma\,\overline{\sum_{\beta,s'}}\frac{\boldsymbol{V}_{2;\alpha\beta}\,\mu_{\beta s'}^{(0)}}{f_\alpha(f_\alpha - ss'f_\beta)}\,\boldsymbol{t}_{\beta s'}^{(0)L}\,, \tag{44}$$

with $\boldsymbol{V}_{2;\alpha\beta} = \sum_i a_i\,u_{\alpha i}\,u_{\beta i}$.

Remark 3: The diagonal elements of the matrix $\boldsymbol{V}_2$ are constrained by $-1 \leq \boldsymbol{V}_{2;\alpha\alpha} = \sum_i a_i\,u_{\alpha i}^2 \leq 1$, since $-1 \leq a_i \leq 1$. Therefore, (42) indicates that when the parameters $\{a_i\}$ are correlated (anticorrelated) with the square components $\{u_{\alpha i}^2\}$ for some α, that mode is more strongly (more weakly) damped. Accordingly, Theorem 2 will distribute the set $\{a_i\}$ in a correlated way with the slowest modes of $\boldsymbol{H}$. This choice reduces the performance measure as much as possible, because it increases the damping of the slowest modes while faster modes are naturally damped by their fast oscillating character (6) [9].

Proposition 4: For an abrupt power loss, $\boldsymbol{\delta P}(t) = \boldsymbol{\delta P}\,\Theta(t)$, on a single bus labeled b, where $\delta P_i = \delta_{ib}\,\delta P$, and under Assumption 2, $\dot{\xi}_\alpha(t)$ is, to leading order in g,

$$\begin{aligned}\dot{\xi}_\alpha(t) = \frac{\mathcal{P}_\alpha}{f_\alpha}e^{-\gamma t/2}\Big[&2s_\alpha\Big(1 + g\frac{\gamma^2}{f_\alpha^2}\boldsymbol{V}_{2;\alpha\alpha}\Big)\\ &-g\gamma t\boldsymbol{V}_{2;\alpha\alpha}\Big(s_\alpha + \frac{\gamma}{f_\alpha}c_\alpha\Big)\Big]\\ &+g\gamma\sum_{\beta\neq\alpha}\frac{\boldsymbol{V}_{2;\alpha\beta}\mathcal{P}_\beta}{\lambda_\alpha - \lambda_\beta}e^{-\gamma t/2}\Big[\frac{\gamma}{f_\beta}s_\beta - \frac{\gamma}{f_\alpha}s_\alpha + c_\alpha - c_\beta\Big]\\ &+\mathcal{O}(g^2)\,,\end{aligned} \tag{45}$$

where $s_\alpha = \sin(f_\alpha t/2)$, $c_\alpha = \cos(f_\alpha t/2)$, and $\mathcal{P}_\alpha$ and f_α are defined below (6).

The proof is based on (42) to (44) and is given in the Appendix.

Proposition 5: For an abrupt power loss, $\boldsymbol{\delta P}(t) = \boldsymbol{\delta P}\,\Theta(t)$, on a single bus labeled b, where $\delta P_i = \delta_{ib}\,\delta P$, and under Assumption 2, the susceptibilities $\alpha_i \equiv \partial\mathcal{M}_b/\partial a_i$ are given by

$$\begin{aligned}\alpha_i = -\frac{g\delta P^2}{2\gamma m_b}\Big[&\sum_{\alpha>1}\frac{u_{\alpha i}^2u_{\alpha b}^2}{\lambda_\alpha}\\ &+\sum_{\substack{\alpha>1,\\ \beta\neq\alpha}}\frac{\gamma^2u_{\alpha i}\,u_{\alpha b}u_{\beta i}\,u_{\beta b}}{(\lambda_\alpha - \lambda_\beta)^2 + 2\gamma^2(\lambda_\alpha + \lambda_\beta)}\Big]\end{aligned} \tag{46}$$

Proof: From (45), to first order in g, one has

$$\begin{aligned}\int_0^\infty\dot{\xi}_\alpha^2(t)\mathrm{d}t = &\frac{\mathcal{P}_\alpha^2}{2\gamma\lambda_\alpha}\left(1 - g\boldsymbol{V}_{2;\alpha\alpha}\right)\\ &-g\gamma\sum_{\beta\neq\alpha}\frac{\boldsymbol{V}_{2;\alpha\beta}\,\mathcal{P}_\alpha\mathcal{P}_\beta}{(\lambda_\alpha - \lambda_\beta)^2 + 2\gamma^2(\lambda_\alpha + \lambda_\beta)} + \mathcal{O}(g^2)\,.\end{aligned} \tag{47}$$

Taking the derivative of (47) with respect to a_i with the definition of $\boldsymbol{V}_{2;\alpha\beta}$ given below (44) and summing over $\alpha > 1$, one obtains (46). ∎

Remark 4: In the vicinity of the homogeneous case $\boldsymbol{M} = m\mathbb{1}$ and $\boldsymbol{\Gamma} = \gamma\mathbb{1}$, summing over every fault location b leads to the vanishing of the second term in (46). One obtains $\sum_b \alpha_i = -g\delta P^2\sum_{\alpha>1}u_{\alpha i}^{(0)2}/(2\gamma\lambda_\alpha^{(0)})$. This follows from the properties of the eigenvectors $\boldsymbol{u}_\alpha^{(0)}$, $\alpha > 1$, of the Laplacian matrix $\boldsymbol{L}$.

IV. OPTIMAL PLACEMENT OF INERTIA AND PRIMARY CONTROL

Having calculated the susceptibilities $\rho_i \equiv \partial\mathcal{M}_b/\partial r_i$ and $\alpha_i \equiv \partial\mathcal{M}_b/\partial a_i$, we are fully equipped to construct our algorithm for the optimal placement of the inertia and primary control.

A. LOCAL OPTIMIZATION

In general, it is not possible to obtain closed-form analytical expressions for the parameters a_i and r_i in determining the optimal placement of the inertia and primary control. Simple optimization algorithms can, however, be constructed that determine how to distribute these parameters to minimize $\mathcal{M}_b$. Theorems 1 and 2 provide two such algorithms for an optimization under Assumptions 1 and 2, respectively. Additionally, Conjecture 1 proposes an algorithm for an optimization under both Assumptions 1 and 2.

Theorem 1: For an abrupt power loss under Assumption 1 and with $\boldsymbol{\Gamma} = \gamma\mathbb{1}$, the optimal distribution of parameters $\{r_i\}$ that minimizes $\mathcal{M}_b$ is obtained as follows.

1) *Compute the sensitivities $\rho_i = \partial\mathcal{M}_b/\partial r_i$ from (32)*
2) *Sort the set $\{\rho_i\}_{i=1,\ldots N}$ in ascending order*
3) *Set $r_i = 1$ for $i = 1,\ldots\mathrm{Int}[N/2]$ and $r_i = -1$ for $i = N - \mathrm{Int}[N/2] + 1,\ldots N$*

The optimal placement of the inertia and primary control is given by

$$m_i = m + \delta m\,r_i\,,\quad d_i = \gamma(m + \delta m\,r_i)\,. \tag{48}$$

The proof is provided in the Appendix.

Theorem 2: For an abrupt power loss under Assumption 2 and with $\boldsymbol{M} = m\mathbb{1}$, the optimal distribution of parameters $\{a_i\}$ that minimizes $\mathcal{M}_b$ is obtained as follows.

1) *Compute the sensitivities $\alpha_i = \partial\mathcal{M}_b/\partial r_i$ from (46).*
2) *Sort the set $\{\alpha_i\}$ in ascending order,*
3) *Set $a_i = 1$ for $i = 1,\ldots\mathrm{Int}[N/2]$ and for $i = N - \mathrm{Int}[N/2] + 1,\ldots N$*

The optimal placement of the primary control is given by

$$d_i = m(\gamma + \delta\gamma\,a_i)\,. \tag{49}$$

Proof: With Proposition 5 and $\boldsymbol{M} = m\mathbb{1}$, we obtain (46). The proof is the same as that for Theorem 1 given in the Appendix but with $\{\alpha_i\}$ instead of $\{\rho_i\}$. ∎

We next propose an algorithmic linear optimization that simultaneously addresses Assumptions 1 and 2 and numerically show that the optimization works well. The main difficulty is that for limited resources, i.e., fixed total inertia

and primary control, one has $\sum_i m_i = N\,m$, $\sum_i d_i = N\,d$ and the latter condition requires $\sum_i a_i r_i = 0$ from (25). This is a quadratic, nonconvex constraint, which makes the problem difficult to solve. The following conjecture presents an algorithm that starts from the distributions $\{r_i\}$ and $\{a_i\}$ from Theorems 1 and 2, which optimize the inertia and primary control placement in the case of an inhomogeneous inertia or damping-to-inertia ratio, respectively. The algorithm orthogonalizes them to satisfy $\sum_i a_i r_i = 0$ while attempting to minimize the unavoidable related increase in $\mathcal{M}_b$.

Conjecture 1 (Combined linear optimization): For an abrupt power loss, under Assumptions 1 and 2, the optimal placement of a fixed total amount of inertia $\sum_i m_i = mN$ and primary control $\sum_i d_i = dN$ that minimizes $\mathcal{M}_b$ is obtained as follows.

1) *Compute the parameters r_i and a_i from Theorems 1 and 2.*
   a) *If N is odd, align the zeros of $\{r_i\}$ and $\{a_i\}$. Let i_{r0} and i_{a0} be the indices of these zeros. Their new common index is*
   $$i_{\rm eqnarray} = \underset{i}{\rm argmin}(r_i\rho_{i_{r0}} + a_i\alpha_{i_{a0}} - r_i\rho_i - a_i\alpha_i)\,.$$
   Interchange the parameter values $r_{i_{r0}} \leftrightarrow r_{i_{\rm eqnarray}}$ and $a_{i_{r0}} \leftrightarrow a_{i_{\rm eqnarray}}$.
   b) *If N is even, do nothing*
2) *If $n \equiv \sum_i r_i a_i = 0$, the optimization is finished.*
3) *Find the set $\mathcal{I} = \{i\,|\,{\rm sgn}(r_i a_i) = {\rm sgn}(n)\}$. To achieve $\sum_i r_i a_i \to 0$, our strategy is set some elements of $\mathcal{I}$ to zero. Since $\sum_i a_i = \sum_i r_i = 0$ must be conserved, this must be accompanied by a simultaneous change in another parameter.*
4) *Find the pair $(a_{i1}, a_{i2} = -a_{i1})$ or $(r_{i1}, r_{i2} = -r_{i1}) \in \mathcal{I}\times\mathcal{I}$ which, when sent to $(0,0)$, induces the smallest increase in the objective function $\mathcal{M}_b$. Send this pair to $(0,0)$. Because this pair has the opposite sign, it does not affect the condition $\sum_i a_i = \sum_i r_i = 0$.*
5) *Go to step # 2.*

Nothing guarantees that this algorithm will optimize the inertia and primary control placement when both are inhomogeneous. However, below we present numerical results indicating that the algorithm is in fact effective.

B. GLOBAL VULNERABILITY

The optimization considered thus far has focused on a single fault in bus b. We are interested, however, in finding the optimal distribution of the inertia and/or primary control for all possible faults. Thus, we introduce the following global vulnerability measure

$$\mathcal{V} = \sum_b \eta_b\,\mathcal{M}_b(\delta P_b)\,, \tag{50}$$

where the sum is taken over all generator buses. The vulnerability measure $\mathcal{V}$ provides a weighted average over all possible fault positions, with the weight η_b accounting for the probability that a fault occurs at b and δP_b accounting for its potential intensity given, e.g., by the rated power of the generator at bus b.

For equiprobable fault locations and for the same power loss everywhere, $\eta_b \equiv 1$, Remark 2 leads to $\partial\mathcal{V}/\partial r_i = 0 + \mathcal{O}(\mu^2)$. Therefore, to leading order, there is no benefit in scaling up the inertia. On the other hand, with Remark 4, we obtain $\partial\mathcal{V}/\partial a_i = -g\delta P^2 \sum_{\alpha>1} u_{\alpha i}^{(0)2}/(2\gamma\lambda_\alpha^{(0)}) + \mathcal{O}(g^2)$. The corresponding optimal placement of primary control can be obtained with Theorem 2, from which we observe that the damping-to-inertia ratios are increased for the buses with large squared components $u_{\alpha i}^{(0)2}$ of the slow modes of $\boldsymbol{L}$ – those with the smallest $\lambda_\alpha^{(0)}$. These modes are displayed in Fig. 1. One concludes that, with a non-weighted vulnerability measure, $\eta_b \equiv 1$ in (50), a homogeneous inertia location is a local optimum for $\mathcal{V}$, for which the damping parameters need to be increased primarily on peripheral buses.

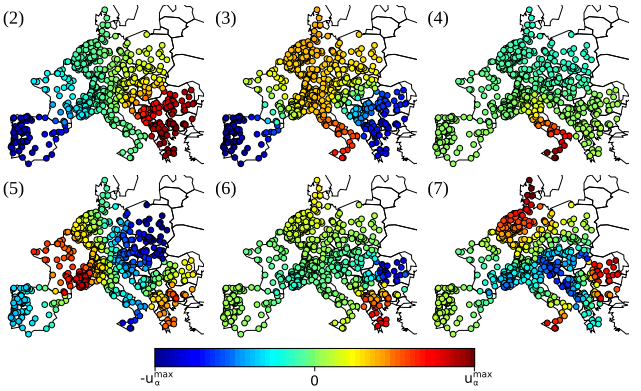

FIGURE 1. Color-coded components of the $\alpha = 2, 3, \ldots 7$ eigenvectors of L. The colors represent the interval $[-u_\alpha^{\max}, u_\alpha^{\max}]$, where $u_\alpha^{\max} = \max_i |u_{\alpha i}^{(0)}|$.

C. OPTIMIZATION OF REALISTIC CONFIGURATIONS

Thus far, our theory has been constructed under the assumption of initially uniform distributions of the inertia and primary control. The theory can be extended to initially nonuniform distributions that are closer to the actual situation in real power grids, under the assumption of almost homogeneous damping-to-inertia ratios, $\gamma_i \equiv d_i/m_i \approx \gamma$. Here, we describe the changes considering such distributions.

With the inertia and primary control varying locally as $m_i = m_{0i} + \delta m_i$, $d_i = d_{0i} + \delta d_i$ but $d_{0i}/m_{0i} \approx \gamma$, unoptimized performance measures $\mathcal{M}_b^{(0)}$ are still given by (18), with however $\lambda_\alpha^{(0)}$ and $\boldsymbol{u}_\alpha^{(0)}$ standing for the eigenvalues and eigenvectors of the matrix $\boldsymbol{L}_{\boldsymbol{M}}^{(\boldsymbol{0})} \equiv \boldsymbol{M}_0^{-1/2}\boldsymbol{L}\boldsymbol{M}_0^{-1/2}$, with $\boldsymbol{M}_0 \equiv {\rm diag}(\{m_{0i}\})$. To optimize the placement of the inertia and primary control, we parametrize them as

$$m_i = m_{0i}\big(1 + \mu r_i\big)\,, \tag{51}$$

$$d_i = d_{0i}\big(1 + \mu r_i\big)\big(1 + g a_i\big)\,, \tag{52}$$

where $\mu = \max_i\big(|\delta m_i|/m_{0i}\big)$. The susceptibilities $\rho_i = \partial\mathcal{M}_b/\partial r_i$ are given by

$$\rho_i = -\frac{\mu\delta P^2\, m_{0i}^{1/2}}{\gamma m_{0b}^{1/2}\sum_k m_{0k}} \sum_{\alpha>1} \frac{u_{\alpha b}^{(0)} u_{\alpha i}^{(0)}}{\lambda_\alpha^{(0)}}\,, \tag{53}$$

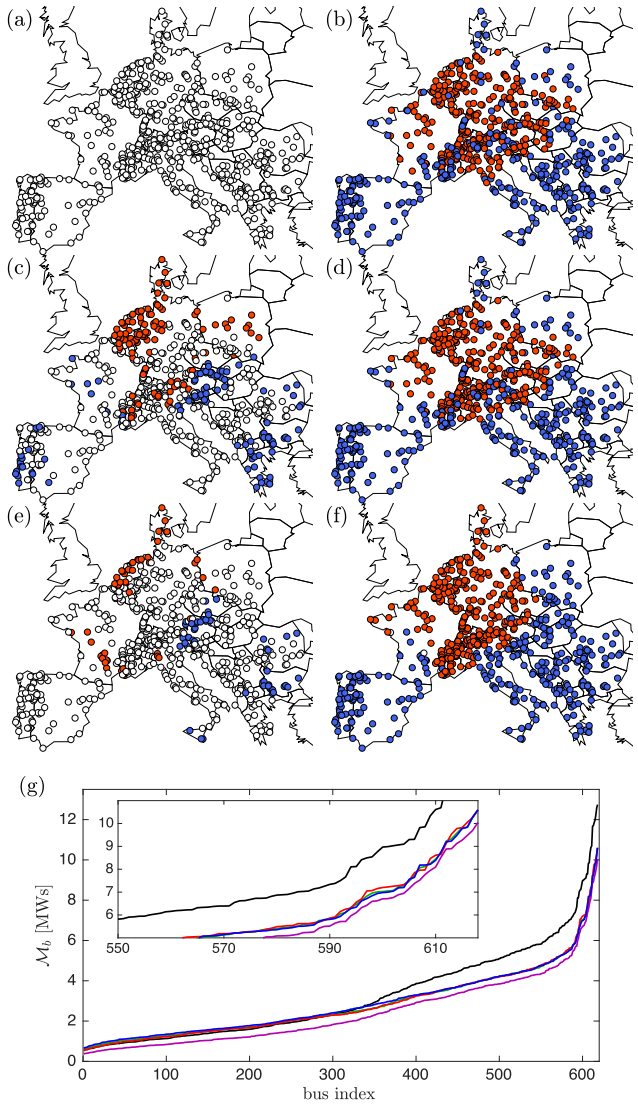

FIGURE 2. Deviation from homogeneous inertia and primary control conditions following the minimization of $\mathcal{V}$ in (50) for different choices of η_b: (a)-(b) $\eta_b \equiv 1$, (c)-(d) $\eta_b = \mathcal{M}_b^{(0)2}$ and (e)-(f) η_b as defined in (55). $r_i = -1, 0, 1$ (left) and $a_i = -1, 0, 1$ (right) are displayed in red, white and blue, respectively. (g) Vulnerability $\mathcal{M}_b$ vs. the fault location (in increasing order of $\mathcal{M}_b$) for the homogeneous model (black) and the optimized models corresponding to (a)-(b) (green line), (c)-(d) (blue line) and (e)-(f) (red line). The purple line shows the best reduction achieved by optimizing r_i and a_i fault-by-fault. The inset highlights the small discrepancies induced by the choice of η_b for the faults with the largest impact. We used $\mu = g = 0.3$.

instead of (32), while $\alpha_i = \partial\mathcal{M}_b/\partial a_i$ are still given by (46), again with the eigenvalues and eigenvectors $\lambda_\alpha^{(0)}$ and $\boldsymbol{u}_\alpha^{(0)}$ of $\boldsymbol{L}_{\boldsymbol{M}}^{(\mathbf{0})}$. The theory can therefore account for inhomogeneous distributions of the inertia, and the condition $d_{0i}/m_{0i} \approx \gamma$ is not unrealistic. Our optimization leads to ratios d_i/m_i varying by a factor of 5-10, similar to their variation for rotating machines in real systems.

D. BUDGET CONSTRAINTS

The employed constraint is that the total inertia and primary control remain constant; $\sum_i a_i = \sum r_i = 0$ is useful, but

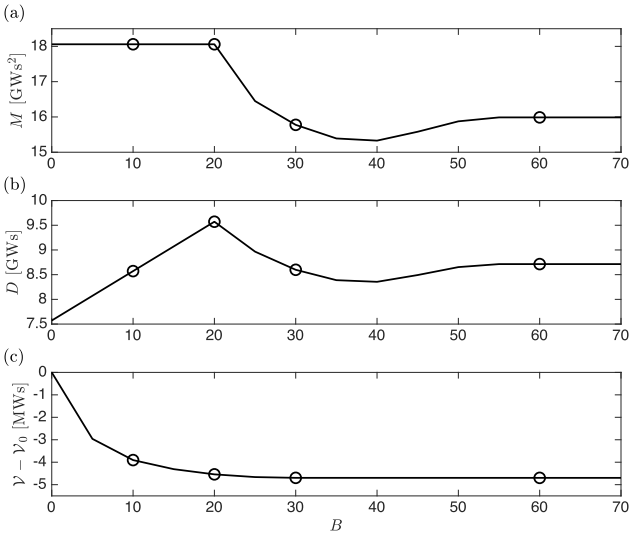

FIGURE 3. Evolution of the total inertia M of the total primary control D and the gain in the global vulnerability $\mathcal{V}$ as the budget B increases. The circles indicate the four budgets corresponding to the distributions in Fig. 4. The initial configuration corresponds to the present situation.

a more realistic constraint would be a financial constraint restricting the available budget to upgrade the system. Therefore, we impose a limited budget to our optimization in the form of a constrained cost function

$$\sum_i \Big(c_i^{\mathrm{m}+}\,\delta m_i^+ + c_i^{\mathrm{d}+}\,\delta d_i^+ + c_i^{\mathrm{m}-}\,\delta m_i^- + c_i^{\mathrm{d}-}\,\delta d_i^- \Big) \leq B\,. \tag{54}$$

Local increases or reductions in the inertia are accompanied by costs $c_i^{\mathrm{m}+}$ or $c_i^{\mathrm{m}-}$, the same is true for local increases and reductions in the primary control, and the total cost is bounded by a predetermined total budget B. The condition (54) is straightforwardly reformulated in terms of r_i and a_i. The resulting optimization problem is more realistic but simultaneously more complex and needs to be solved numerically.

V. NUMERICAL INVESTIGATIONS

In [9] and [26], we constructed a synthetic, numerical model of the synchronous power grid of continental Europe, with 3809 buses, 618 of which are generator buses. We use this model to numerically validate the main results derived above. To align with our theoretical results, we first remove the inertialess buses via a Kron reduction [30].

We optimize the placement of the inertia and primary control in the continental European grid. We numerically investigate the response of the grid for localized contingencies and verify the reduction in the system vulnerability. For every fault location b, the system encounters an abrupt power loss described by $P_b(t) = P_b - \delta P\,\Theta(t)$, with $\delta P = 100$ [MW]. We integrate the system dynamics described in (1) and compute the measure $\mathcal{M}$ defined in (13).

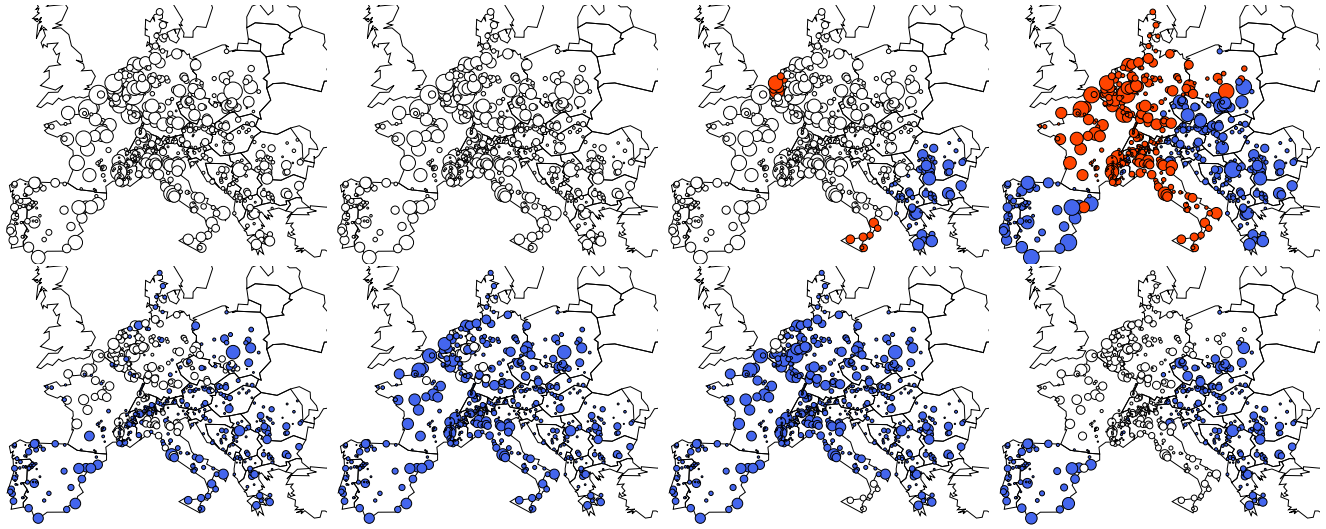

FIGURE 4. From left to right, the optimal enhancement in the inertia (top) and primary control (bottom) as the budget B increases. The areas of the disks are proportional to the amount of inertia or of primary control. The increases and decreases are highlighted in blue and red, respectively. The initial configuration corresponds to the present situation of the dynamical resources in Europe.

A. UNIFORM INITIAL CONFIGURATION

We homogenize the distribution of the inertia with $m_i = 29.22$ MWs^2 and that of the primary control with $d_i = 12.25$ MWs so that the total amounts remain the same as those in the original synthetic model.

In the previous section, we argued that a homogeneously distributed inertia, together with an increased primary control on the slowest eigenmodes of the network Laplacian minimize the global vulnerability measure $\mathcal{V}$ of (50) for $\eta_b \equiv 1$. This conclusion is confirmed numerically in Fig. 2 (a) and (b). The optimal placement of the primary control displayed in panel (b) decreases $\mathcal{V}$ by more than 12% with respect to the homogeneous case.

Setting $\eta_b \equiv 1$ in (50) is convenient mathematically but treats all faults equally, regardless of their impact. One may instead adapt η_b to obtain the inertia and primary control distributions that reduce the impact of the strongest faults with the largest $\mathcal{M}_b$. Here, we employ two different methods: first setting $\eta_b = \mathcal{M}_b^{(0)2}$ and second with

$$\eta_b = \begin{cases} 1\,, & \text{if } \mathcal{M}_b^{(0)} > \mathcal{M}_{\text{thres}}, \\ 0\,, & \text{otherwise.} \end{cases} \tag{55}$$

The corresponding geographical distributions of the inertia and primary control redistribution parameters r_i and a_i are shown in Fig. 2 (c) and (d) and Fig. 2 (e) and (f), respectively. Compared to the choice of $\eta_b \equiv 1$ [Fig. 2 (a) and (b)], we obtain small differences. More importantly, the impact of various choices of η_b on $\mathcal{M}_b$ is almost negligible, as shown in Fig. 2 (g). In all cases, our optimization algorithm reduces the impact of the strongest faults, with little or no influence on the faults with weakest impact on grid stability.

Most interestingly, our three choices of η_b are close to optimal, especially when considering the strongest faults. This can be seen in Fig. 2 (g), where the purple line shows the maximal obtainable reduction when the inertia and primary control distributions are optimized individually fault-by-fault, i.e., with a different redistribution for each fault. The inset of Fig. 2 (g) shows that for the strongest fault, the three considered choices of η_b lead to reductions in $\mathcal{M}_b$ that are very close to the maximal value. We conclude that rather generically, the inertia is optimally distributed homogeneously, while the primary control should be preferentially located on the slow modes of the grid Laplacian.

B. BUDGET-CONSTRAINED OPTIMIZATION

The presented numerical results illustrate the validity and power of our theory. We next consider the two more realistic situations of (i) the current distribution of inertia in the European transmission grid and (ii) a possible future configuration of a European transmission grid with strongly reduced inertia, corresponding to an advanced stage of the energy transition with a large penetration of inverter-connected new renewable sources.

Fig. 3 shows the evolution of the total inertia and primary control connected to the system as a function of the available budget B for situation (i) corresponding to the current configuration of the European transmission grid. Most of the optimization is obtained relatively fast, and only by adding primary control. We find that 96 % of the effect is readily obtained for $B = 20$ only by adding primary control with no change in the inertia. Furthermore, achieving the maximal optimization requires an increase in the budget to $B = 50$. An inertia redistribution and/or addition is essentially useless: it only allows a gain of a few percent in the optimization but is associated with a high cost.

Fig. 4 shows the optimal system enhancement for four different values of the budget B corresponding from left to

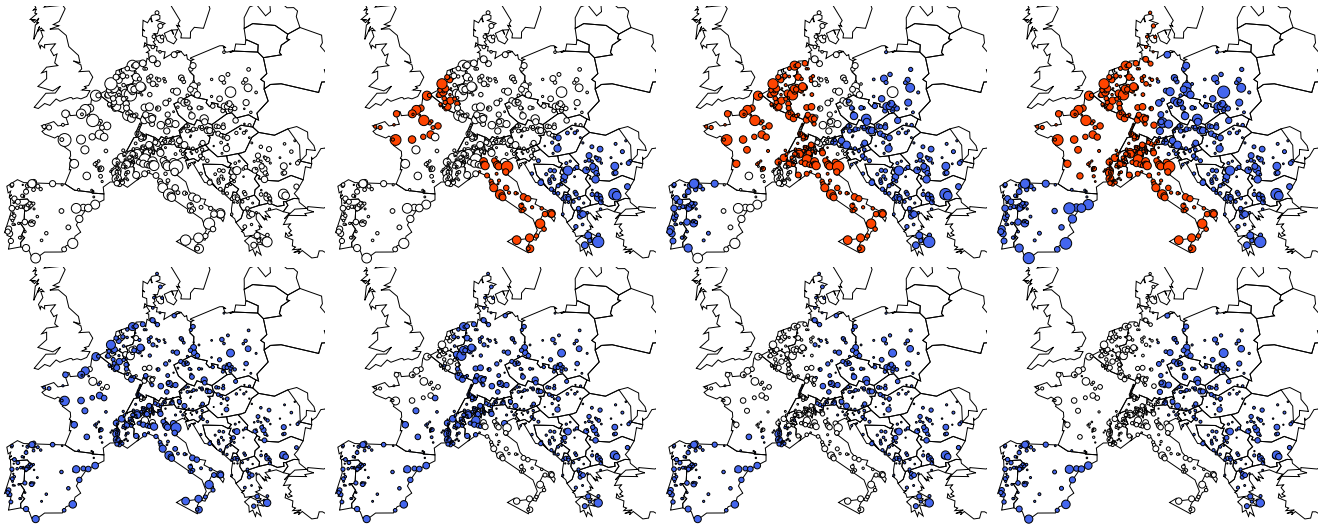

FIGURE 5. From left to right, the optimal enhancement in the inertia (top) and primary control (bottom) as the budget B increases. The areas of the disks are proportional to the amount of inertia or primary control. Increases and decreases are highlighted in blue and red, respectively. The initial configuration represents a later stage of the energy transition, and contributions from nuclear and coal-fired power plants are significantly reduced.

right to the four circles in Fig. 3. The primary control is, up to $B = 20$, increased in the periphery of the grid. This qualitatively corroborates the above arguments that the primary control should be increased on the slow modes of the grid Laplacian. As a matter of fact, it is expected that these slow modes dominantly reside in the grid periphery [9]. The inertia is only redistributed for a higher budget; however, as already mentioned, this occurs with little decrease in the performance measure.

We finally consider a potential future European transmission grid, where nuclear and coal-fired power stations are partially dismantled and substituted with inertialess new renewable sources. Accordingly, we reduce the corresponding inertia by a factor of three, $m_i \to m_i/3$. While this scenario is unlikely to be realized in the future, it allows us to investigate a power grid with strongly reduced inertia. Fig. 5 shows that the optimization leads to qualitatively similar results as those for the current configuration of the European transmission grid – it seems more important to redistribute the primary control than the inertia. Nevertheless, from a quantitative point of view, this situation with more inverter-connected production seems to require an inertia redistribution even with a lower budget. An interesting study beyond the scope of the present paper would be to quantitatively investigate what penetration level of new renewable resources requires a redistribution and/or an increase in the inertia resources.

All of these numerical data correspond to the cost parameters $c_i^{\mathrm{m}+} = 1\ (\mathrm{MWs}^2)^{-1}$, $c_i^{\mathrm{m}-} = 0.1\ (\mathrm{MWs}^2)^{-1}$, $c_i^{\mathrm{d}+} = 1\ (\mathrm{MWs})^{-1}$ and $c_i^{\mathrm{d}-} = 0.1\ (\mathrm{MWs})^{-1}$ in (54). This arbitrary choice takes into account that installing resources is more expensive than dismantling them. We have checked that our conclusions do not change qualitatively for $c_i^{\mathrm{m}\pm}/c_i^{\mathrm{d}\pm} \in [0.1, 10]$, and only an increase in B occurs when the primary control costs are increased with respect to the inertia costs. In all cases, the primary control increase and its targeted distribution provide most of the maximal possible optimization, with only a small, expensive contribution arising from the inertia redistribution.

VI. CONCLUSION

To find the optimal placement of inertia and primary control in electric power grids is a problem of paramount importance. Here, we have realized an important step forward in constructing a perturbative analytical theory for this problem. In this approach, both the inertia and primary control are limited resources, whose placement needs to be optimized simultaneously. Most importantly, our method goes beyond the usual assumption of a constant damping-to-inertia ratio. In our approach, the inertia and primary control can vary spatially independently.

Our results indicate that grid stability as quantified by the performance measures of (13) and (50) is improved dominantly by an appropriate increase and geographical distribution of the primary control resources. The primary control should in particular be reinforced on buses that support the slower modes of the network Laplacian. We found, rather surprisingly, that the inertia plays a very limited role in the optimization of our performance measures. Nonetheless, comparing Figs. 4 and 5 seems to indicate that in power grids with increased penetration of inertialess, inverter-connected production, the inertia redistribution becomes more important. Future works should investigate in detail the critical amount of inertialess production for which a change in behavior will occur.

Our results emphasize the importance of simultaneously optimizing the inertia and primary control. In particular, the latter should also be considered as a control variable,

which may be a shortcoming of Ref. [6]. Finally, it would be interesting to compare our method with the methods of Refs. [4], [8], where both the inertia and primary control are control variables.

One limitation of our theory is that it considers only the first order in perturbation theory. Future work should try to extend this approach to the next order in perturbation theory or include the presented results in an iterative algorithm, for instance, along the lines of Ref. [4]. Work in this direction is in progress.

APPENDIX

Proof of Proposition 4:

The proof follows the same steps as those for Proposition 1. The calculations are rather tedious though algebraically straightforward. In the following, we describe the calculation steps. Assuming that $\boldsymbol{H}$ can be diagonalized as $\boldsymbol{t}^R \boldsymbol{\mu} \boldsymbol{t}^L$, where $\boldsymbol{\mu} \equiv \mathrm{diag}(\{\mu_{\alpha s}\})$ and $\boldsymbol{t}^{R,L}$ are matrices containing the right and left eigenvectors of $\boldsymbol{H}$, the problem is resolved by:

1) changing variables $\boldsymbol{\chi} \equiv \boldsymbol{t}^L[\boldsymbol{\xi}^\top \dot{\boldsymbol{\xi}}^\top]^\top$ to diagonalize (36), as

$$\dot{\boldsymbol{\chi}} = \boldsymbol{\mu}\boldsymbol{\chi} + \boldsymbol{t}^L \begin{bmatrix} \mathbb{0}_{N\times 1} \\ \boldsymbol{\mathcal{P}} \end{bmatrix} \equiv \boldsymbol{\mu}\boldsymbol{\chi} + \tilde{\boldsymbol{\mathcal{P}}}\,; \tag{56}$$

2) solving (56) as

$$\chi_{\alpha\pm} = -\frac{\tilde{\mathcal{P}}_{\alpha\pm}}{\mu_{\alpha\pm}}\left(1 - e^{\mu_{\alpha\pm} t}\right),\ \forall \alpha > 1\,; \tag{57}$$

3) and obtaining $\dot{\xi}_\alpha$ via the inverse transformation $[\boldsymbol{\xi}^\top \dot{\boldsymbol{\xi}}^\top]^\top = \boldsymbol{t}^R \boldsymbol{\chi}$.

These three steps are carried out with the approximate expressions $\boldsymbol{t}^{R,L} = \boldsymbol{t}^{R,L(0)} + g\boldsymbol{t}^{R,L(1)}$ and $\mu_{\alpha\pm} = \mu^{(0)}_{\alpha\pm} + g\mu^{(1)}_{\alpha\pm}$ obtained with the first-order corrections in g presented in (42)–(44). One obtains

$$\begin{aligned}\begin{bmatrix} \xi_\alpha \\ \dot{\xi}_\alpha \end{bmatrix} &= \begin{bmatrix} 1 & 1 \\ \mu^{(0)}_{\alpha+} & \mu^{(0)}_{\alpha-} \end{bmatrix}\begin{bmatrix} \chi_{\alpha+} \\ \chi_{\alpha-} \end{bmatrix} - \frac{g\gamma \boldsymbol{V}_{2;\alpha\alpha}}{f_\alpha^2}\begin{bmatrix} \mu^{(0)}_{\alpha+} & \mu^{(0)}_{\alpha-} \\ \lambda_\alpha & \lambda_\alpha \end{bmatrix} \\ &\quad \begin{bmatrix} \chi^{(0)}_{\alpha+} \\ \chi^{(0)}_{\alpha-} \end{bmatrix} - g\gamma \sum_{\beta\neq\alpha} \frac{\boldsymbol{V}_{2;\alpha\beta}}{\lambda_\alpha - \lambda_\beta} \\ &\quad \begin{bmatrix} \mu^{(0)}_{\beta+} & \mu^{(0)}_{\beta-} \\ \mu^{(0)2}_{\beta+} & \mu^{(0)2}_{\beta-} \end{bmatrix}\begin{bmatrix} \chi^{(0)}_{\beta+} \\ \chi^{(0)}_{\beta-} \end{bmatrix} + \mathcal{O}(g^2)\,, \end{aligned} \tag{58}$$

with

$$\begin{aligned}\chi_{\alpha\pm} = &-\frac{1}{\mu^{(0)}_{\alpha\pm}}\left[\tilde{\mathcal{P}}^{(0)}_{\alpha\pm} + g\tilde{\mathcal{P}}^{(1)}_{\alpha\pm} - g\frac{\mu^{(1)}_{\alpha\pm}\tilde{\mathcal{P}}^{(0)}_{\alpha\pm}}{\mu^{(0)}_{\alpha\pm}}\right]\left(1 - e^{\mu^{(0)}_{\alpha\pm} t}\right) \\ &+ gt\frac{\mu^{(1)}_{\alpha\pm}\tilde{\mathcal{P}}^{(0)}_{\alpha\pm}}{\mu^{(0)}_{\alpha\pm}} e^{\mu^{(0)}_{\alpha\pm} t} + \mathcal{O}(g^2)\,, \end{aligned} \tag{59}$$

where

$$\begin{aligned}\begin{bmatrix} \tilde{\mathcal{P}}^{(0)}_{\alpha+} \\ \tilde{\mathcal{P}}^{(0)}_{\alpha-} \end{bmatrix} &= \frac{i}{f_\alpha}\begin{bmatrix} \mu^{(0)}_{\alpha-} & -1 \\ -\mu^{(0)}_{\alpha+} & 1 \end{bmatrix}\begin{bmatrix} 0 \\ \mathcal{P}_\alpha \end{bmatrix}, \\ \begin{bmatrix} \tilde{\mathcal{P}}^{(1)}_{\alpha+} \\ \tilde{\mathcal{P}}^{(1)}_{\alpha-} \end{bmatrix} &= \frac{i\gamma}{f_\alpha}\Bigg(-\frac{\boldsymbol{V}_{2;\alpha\alpha}}{f_\alpha^2}\begin{bmatrix} \lambda_\alpha & -\mu^{(0)}_{\alpha-} \\ -\lambda_\alpha & \mu^{(0)}_{\alpha+} \end{bmatrix}\begin{bmatrix} 0 \\ \mathcal{P}_\alpha \end{bmatrix} \\ &\quad + \sum_{\beta\neq\alpha}\frac{\boldsymbol{V}_{2;\alpha\beta}}{(\lambda_\alpha - \lambda_\beta)}\begin{bmatrix} \lambda_\beta & -\mu^{(0)}_{\alpha+} \\ -\lambda_\beta & \mu^{(0)}_{\alpha-} \end{bmatrix}\begin{bmatrix} 0 \\ \mathcal{P}_\beta \end{bmatrix}\Bigg). \end{aligned} \tag{60}$$

(45) is obtained from (58) by applying trigonometric identities. ■

Proof of Theorem 1: To leading order in $\mu = \delta m/m$, this optimization problem is equivalent to the following linear programming problem [31]

$$\min_{\{r_i\}} \sum_i \rho_i r_i\,, \tag{61}$$

$$\text{s.t. } |r_i| \leq 1\,, \tag{62}$$

$$\sum_i r_i = 0\,. \tag{63}$$

The problem is solved by the Lagrange multipliers method with the Lagrangian function

$$\mathcal{L} = \sum_{i=1}^N \rho_i r_i + \sum_{i=1}^N \varepsilon_i(r_i^2 - 1) + \varepsilon_0 \sum_{i=1}^N r_i\,, \tag{64}$$

where ε_i and ε_0 are Lagrange multipliers. We obtain

$$\frac{\partial \mathcal{L}}{\partial r_i} = \rho_i + 2\varepsilon_i r_i + \varepsilon_0 = 0\,, \quad \forall i\,. \tag{65}$$

The solution must satisfy the Karush-Kuhn-Tucker (KKT) conditions [31] and in particular the complementary slackness (CS) condition, which imposes that either $\varepsilon_i = 0$ or $r_i = \pm 1$, $\forall i$. The former choice generally leads to a contradiction. From (65) and dual feasibility conditions, one obtains

$$\varepsilon_i = -\frac{\varepsilon_0 + \rho_i}{2r_i} \geq 0\,. \tag{66}$$

This imposes that $r_i = -\mathrm{sgn}(\varepsilon_0 + \rho_i)$. To ensure that $\sum_i r_i = 0$ is satisfied, ε_0 is set to the negative of the median value of ρ_i. If the number of bus N is odd, r_i corresponding to the median value of ρ_i is set to zero. ■

REFERENCES

[1] A. Ulbig, T. S. Borsche, and G. Andersson, "Impact of low rotational inertia on power system stability and operation," *IFAC Proc. Vols.*, vol. 47, no. 3, pp. 7290–7297, 2014.

[2] M. Milligan, B. Frew, B. Kirby, M. Schuerger, K. Clark, D. Lew, P. Denholm, B. Zavadil, M. O'Malley, and B. Tsuchida, "Alternatives no more: Wind and solar power are mainstays of a clean, reliable, affordable grid," *IEEE Power Energy Mag.*, vol. 13, no. 6, pp. 78–87, Nov./Dec. 2015.

[3] W. Winter, K. Elkington, G. Bareux, and J. Kostevc, "Pushing the limits: Europe's new grid: Innovative tools to combat transmission bottlenecks and reduced inertia," *IEEE Power Energy Mag.*, vol. 13, no. 1, pp. 60–74, Jan./Feb. 2015.

[4] T. S. Borsche, T. Liu, and D. J. Hill, "Effects of rotational Inertia on power system damping and frequency transients," in *Proc. IEEE 54th Annu. Conf. Decis. Control (CDC)*, Dec. 2015, pp. 5940–5946.

[5] A. Mešanović, U. Münz, and C. Heyde, "Comparison of H_∞, H_∞, and pole optimization for power system oscillation damping with remote renewable generation," *IFAC-PapersOnLine*, vol. 49, no. 27, pp. 103–108, 2016.
[6] B. K. Poolla, S. Bolognani, and F. Dörfler, "Optimal placement of virtual inertia in power grids," *IEEE Trans. Autom. Control*, vol. 62, no. 12, pp. 6209–6220, Dec. 2017.
[7] F. Paganini and E. Mallada, "Global performance metrics for synchronization of heterogeneously rated power systems: The role of machine models and inertia," in *Proc. 55th Annu. Allerton Conf. Commun., Control, Comput.*, Oct. 2017, pp. 324–331.
[8] T. Borsche and F. Dörfler, "On placement of synthetic inertia with explicit time-domain constraints," 2017, *arXiv:1705.03244*. [Online]. Available: https://arxiv.org/abs/1705.03244
[9] L. Pagnier and P. Jacquod, "Inertia location and slow network modes determine disturbance propagation in large-scale power grids," *PLoS ONE*, vol. 14, no. 3, 2019, Art. no. e0213550.
[10] G. W. Stewart and J.-G. Sun, *Matrix Perturbation Theory*. Boston, MA, USA: Academic, 1990.
[11] D. McIntyre, *Quantum Mechanics*. San Francisco, CA, USA: Addison-Wesley, 2012.
[12] T. Coletta and P. Jacquod, "Performance measures in electric power networks under line contingencies," *IFAC PapersOnLine*, vol. 51, no. 23, pp. 337–342, 2018.
[13] M. Pirani, J. Simpson-Porco, and B. Fidan, "System-theoretic performance metrics for low-inertia stability of power networks," in *Proc. 56th Annu. Conf. Decis. Control (CDC)*, Dec. 2017, pp. 5106–5111.
[14] L. Guo, C. Zhao, and S. H. Low, "Graph Laplacian spectrum and primary frequency regulation," 2018, *arXiv:1803.03905*. [Online]. Available: https://arxiv.org/abs/1803.03905
[15] M. Porfiri and M. Frasca, "Robustness of synchronization to additive noise: How vulnerability depends on dynamics," *IEEE Trans. Control Netw. Syst.*, vol. 6, no. 1, pp. 375–387, Mar. 2018.
[16] P. Jacquod and L. Pagnier, "Optimal placement of inertia and primary control in high voltage power grids," in *Proc. 53rd Conf. Inf. Sci. Syst.*, Mar. 2019, pp. 1–6.
[17] J. Machowski, J. Bialek, and J. R. Bumby, *Power System Dynamics: Stability and Control*, 2nd ed. Hoboken, NJ, USA: Wiley, 2008.
[18] T. Coletta, B. Bamieh, and P. Jacquod, "Transient performance of electric power networks under colored noise," in *Proc. IEEE Conf. Decis. Control (CDC)*, 2018, pp. 6163–6167.
[19] E. Tegling, B. Bamieh, and D. F. Gayme, "The price of synchrony: Evaluating the resistive losses in synchronizing power networks," *IEEE Trans. Control Netw. Syst.*, vol. 2, no. 3, pp. 254–266, Sep. 2015.
[20] M. Fardad, F. Lin, and M. R. Jovanović, "Design of optimal sparse interconnection graphs for synchronization of oscillator networks," *IEEE Trans. Autom. Control*, vol. 59, no. 9, pp. 2457–2462, Sep. 2014.
[21] T. W. Grunberg and D. F. Gayme, "Performance measures for linear oscillator networks over arbitrary graphs," *IEEE Trans. Control Netw. Syst.*, vol. 5, no. 1, pp. 456–468, Mar. 2018.
[22] M. Siami and N. Motee, "Fundamental limits and tradeoffs on disturbance propagation in linear dynamical networks," *IEEE Trans. Autom. Control*, vol. 61, no. 12, pp. 4055–4062, Dec. 2016.
[23] M. Tyloo, T. Coletta, and P. Jacquod, "Robustness of synchrony in complex networks and generalized Kirchhoff indices," *Phys. Rev. Lett.*, vol. 120, Feb. 2018, Art. no. 084101.
[24] Y. Guo and T. H. Summers, "A performance and stability analysis of low-inertia power grids with stochastic system inertia," 2019, *arXiv:1903.00635*. [Online]. Available: https://arxiv.org/abs/1903.00635
[25] D. Klein and M. Randić, "Resistance distance," *J. Math. Chem.*, vol. 12, p. 81, Dec. 1993.
[26] M. Tyloo, L. Pagnier, and P. Jacquod, "The key player problem in complex oscillator networks and electric power grids: Resistance centralities identify local vulnerabilities," 2018, *arXiv:1810.09694*. [Online]. Available: https://arxiv.org/abs/1810.09694
[27] I. Gutman and B. Mohar, "The Quasi–Wiener and the Kirchhoff indices coincide," *J. Chem. Inf. Comput. Sci.*, vol. 36, no. 2, pp. 982–985, 1996.
[28] H.-Y. Zhu, D. J. Klein, and I. Lukovits, "Extensions of the Wiener number," *J. Chem. Inf. Comput. Sci.*, vol. 36, no. 2, pp. 420–428, 1996.
[29] L. V. Gambuzza, A. Buscarino, L. Fortuna, M. Porfiri, and M. Frasca, "Analysis of dynamical robustness to noise in power grids," *IEEE J. Emerg. Sel. Topics Circuits Syst.*, vol. 7, no. 3, pp. 413–421, Sep. 2017.
[30] F. Dörfler and F. Bullo, "Kron reduction of graphs with applications to electrical networks," *IEEE Trans. Circuits Syst. I, Reg. Papers*, vol. 60, no. 1, pp. 150–163, Jan. 2013.
[31] D. Bertsimas and J. N. Tsitsiklis, *Introduction to Linear Optimization*. Belmont, MA, USA: Athena Scientific 1997.

LAURENT PAGNIER (M'17) received the M.S. and Ph.D. degrees in theoretical physics from EPFL, Lausanne, Switzerland, in 2014 and 2019, respectively. He is currently a Postdoctoral Researcher with the Electrical Energy Efficiency Group, University of Applied Sciences of Western Switzerland, Sion, Switzerland. His research interest includes development of new renewable energy sources and their effects on transmission grids.

PHILIPPE JACQUOD (M'16) received the Diploma degree in theoretical physics from ETHZ, Zürich, Switzerland, in 1992, and the Ph.D. degree in natural sciences from the University of Neuchâtel, Switzerland, in 1997. From 2003 to 2005, he was an Assistant Professor with the Theoretical Physics Department, University of Geneva, Switzerland, and a Professor with the Physics Department, The University of Arizona, Tucson, USA, from 2005 to 2013. He is currently a Professor with the Engineering Department, University of Applied Sciences of Western Switzerland, Sion, Switzerland, and a joint appointment at the Department of Quantum Matter Physics, University of Geneva. He has published more than 100 articles in international journals, books, and conference proceedings. His main research interest includes power systems and how they evolve as the energy transition unfolds.